

# Control of the Supersaturation in the CF–PVT Process for the Growth of Silicon Carbide Crystals: Research and Applications

Didier Chaussende,<sup>\*,†</sup> Magali Ucar,<sup>‡,§</sup> Laurent Auvray,<sup>†,‡</sup> Francis Baillet,<sup>§</sup> Michel Pons,<sup>§</sup> and Roland Madar<sup>†</sup>

Laboratoire des Matériaux et du Génie Physique, INPGrenoble-CNRS, BP46, 38402 Saint Martin d'Hères, France, NOVASiC Savoie Technolac, BP 267, 73375 Le Bourget du Lac Cedex, France, and Laboratoire de Thermodynamique et Physico-Chimie Métallurgiques, INPGrenoble-CNRS, BP 75, 38402 Saint Martin d'Hères, France

Received January 10, 2005; Revised Manuscript Received March 29, 2005

**ABSTRACT:** In the classical sublimation growth of silicon carbide (SiC) single crystals, the supersaturation in the surrounding of the seed is mainly controlled by pressure and temperature distributions within the growth cavity. Precise control of the supersaturation is difficult, especially if it needs to be adjusted during the process. In the first part of the paper, an experimental study performed in a continuous feed–physical vapor transport reactor (CF–PVT) is shown. This process combines CVD for the feeding of the SiC source and PVT for the growth of the single crystal. It is shown that the feeding gas flow rate (TMS diluted in argon) and/or the temperature allow precise control of the supersaturation close to the seed, much more easily than in the classical sublimation process. In the second part of the paper, the application of the supersaturation control to SiC polytype engineering is demonstrated.

## 1. Introduction

Single crystalline silicon carbide (SiC) ingots are currently grown by the seeded sublimation method (PVT for physical vapor transport; see for example refs 1–5). This technique has proven its ability for processing large dimension boules, up to 100 mm both in diameter and in length.<sup>6</sup> Moreover, the possibility to eliminate different kinds of structural defects and thus to obtain wafers of small size with a dislocation density near  $100\text{ cm}^{-2}$  has been recently reported by using a sequence of growth runs along two crystallographic directions.<sup>7</sup> Another technique of interest is the high-temperature chemical vapor deposition (HTCVD), which is able to grow very high purity material.<sup>8</sup> Although these techniques have reached a maturity level high enough to be industrialized, they would benefit by being further improved so as to get longer ingots with higher purity and higher structural quality. Along this line, the continuous feed–physical vapor transport (CF–PVT) method was recently proposed as a new process concept to grow large boules of high purity. CF–PVT offers the advantage to combine the maturity of PVT for single-crystal growth and HTCVD for continuous feeding of the high-purity polycrystalline SiC source. On the basis of a coupled approach involving both numerical simulation and experiments, this new concept has been validated.<sup>9</sup>

In the growth of SiC from the vapor phase, the precise control of the mass transfer within the growth cavity is one of the key parameters as it fixes the supersaturation close to the seed. Control of this transfer thus governs

more or less closely the nature of the polytype and the occurrence of different kinds of defects.<sup>10–12</sup> Most of the defects are formed during the initial stage of the growth.<sup>13</sup> In the classical sublimation method, the mass transfer is controlled by pressure and temperature distributions within the crucible. A precise control of the supersaturation is difficult, especially if it needs to be adjusted during the process. The perfect mass transfer management remains a challenge first for the nucleation step of the layer, for example, in the case of heteropolytypic growth, and second for long-lasting experiments.

The aim of this paper is to improve the knowledge of the phenomena occurring during the transfer of SiC across porous graphite foams, which delimitate the CVD chamber from the sublimation chamber in the CF–PVT process. In the first part of the paper, the study of supersaturation will be shown, and the optimal experimental parameters will be discussed. In the second part of the paper, these results will be applied to two examples: homoepitaxial growth of bulk 2 in. 4H–SiC and heteroepitaxial growth of bulk 3C–SiC on 4H–SiC seeds.

## 2. Experimental Details

The experimental setup is a modified sublimation reactor, with inductive heating and a water-cooled quartz tube. The crucible is totally made of graphite and thermally insulated with graphite felts. A schematic representation of the crucible is presented in Figure 1.

It is composed of three main graphite pieces: the heating element, the sublimation chamber, and the CVD chamber, which delimitate the three “reaction zones”. (1) The first one is *the feeding zone* where the polycrystalline source is formed from tetramethylsilane (TMS) diluted in argon. (2) The second one is *the transfer zone* consisting of highly porous graphite foam, which supports the CVD deposit and allows SiC transfer to the sublimation area. (3) The third one is *the sublimation zone* containing the SiC seed stucked on the top of the crucible.

\* Corresponding author: Tel: + 33 4 76 82 63 15. Fax: + 33 4 76 82 63 94. E-mail: didier.chaussende@inpg.fr.

† Laboratoire des Matériaux et du Génie Physique, INPGrenoble-CNRS.

‡ NOVASiC Savoie Technolac.

§ Laboratoire de Thermodynamique et Physico-Chimie Métallurgiques, INPGrenoble-CNRS.

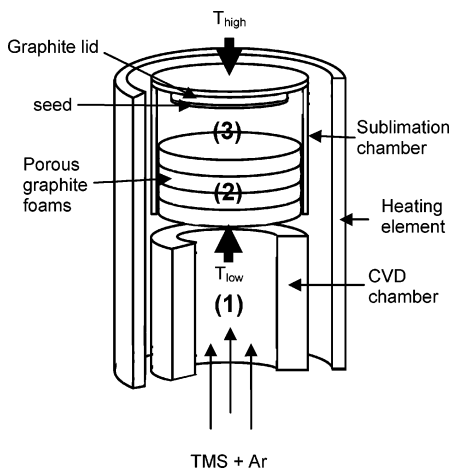


**Figure 1.** CF-PVT crucible setup. Pyrometric measurement. (1) Feeding zone, (2) transfer zone, and (3) sublimation zone.

The crucible is indirectly heated as the maximum power dissipation from the induction coil is reached in the heating element. The three reaction zones are thus mainly heated by radiation and convection phenomena. During the process, the monitored parameters are temperature, pressure, and gas flow rates. The growth pressure is always lower than 5 mbar. Temperature measurements are performed by optical pyrometers on the top of the crucible ( $T_{\text{high}}$ ) and on the graphite foam in the feeding area ( $T_{\text{low}}$ ). The temperature monitoring is linked to  $T_{\text{high}}$ . This study was carried out in a temperature range varying from 1850 to 2050 °C ( $T_{\text{high}}$ ). The argon flow rate, 400 sccm, is kept constant for all experiments presented in this paper. Different TMS flow rates are investigated, from 16 to 64 sccm, corresponding to TMS/Ar ratios of 0.04 and 0.16. In the following, we will refer to the TMS/Ar ratio. We selected the TMS-Ar chemical system on the basis of a previous work.<sup>14</sup> Indeed, it has been demonstrated that this system could lead to the best SiC deposition yield at high temperature in the CVD area. The use of chlorinated precursors were promising for the CVD step but appeared to be very harmful concerning the SiC transfer by sublimation in both the transfer zone and the sublimation zone.

For this study, the transfer zone is composed of four similar pieces of graphite foam stacked one over the other. The porosity of the foam is about 97%. The graphite foams are numbered 1 to 4; 1 is the lower foam, which is fed by the CVD step, and 4 is the upper one (Figure 1).

In the first experimental section (section 3), each graphite foam is weighted before and after the experiment to get a quantitative estimation of mass transfer. The same is done for the sublimation crucible lid. Note that no seed is used in these cases. SiC crystals directly grow on the graphite lid. Its surface is systematically polished prior to the experiments to start with the same surface and to compare the nucleation trends. TMS is injected once the thermal equilibrium of the crucible is reached. It is important to note that all the measurements are done for deposition times shorter than 3 h. For longer growth time, modifications of geometrical parameters such as the graphite foam porosity should be taken into account in the mass transfer study.

In the second part of the paper (section 5), (0001) oriented 4H-SiC seed are glued on the graphite lid. We used "epi-ready" Si-face from the NOVASiC StepSiC polishing as starting surface. A piece of silicon is placed between the graphite foam to maintain the Si partial pressure at the beginning of the experiments and then to prevent seed graphitization.

### 3. Results

#### 3.1. Temperature Distribution in the Crucible.

First, it is important to precisely determine how thermal fields are distributed inside the crucible. Those have been calculated taking into account electromagnetics,

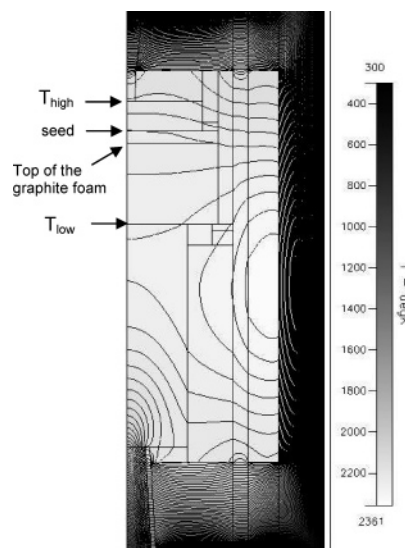


**Figure 2.** Temperature distribution (K) obtained from numerical simulation.

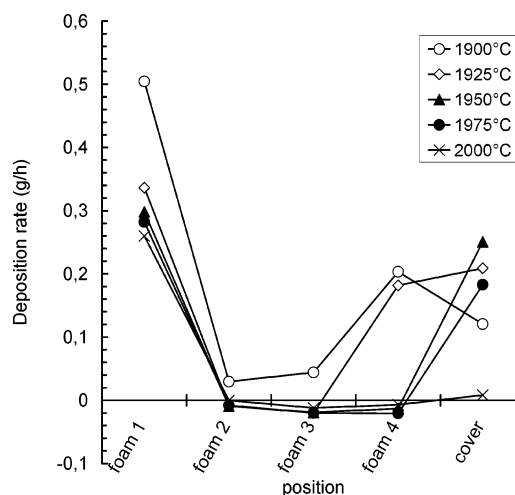


**Figure 3.** Weight gains or losses for the different foams and for the crucible cover as a function of temperature. The TMS/Ar ratio was kept about 0.08. The graphite foams were numbered 1 to 4. 1 was the lower foam, which was fed from the CVD step, and 4 was the upper one.

fluid mechanics, and heat transfer and are shown for a half-crucible in Figure 2. Details on the models and data used in the numerical simulation have been already reported in a previous work.<sup>9</sup> As an example, temperatures calculated in Figure 2 are 1926 °C for  $T_{\text{high}}$ , 1964 °C for the seed, 1971 °C for the top of the graphite foam, and 2001 °C for the bottom of the graphite foam ( $T_{\text{low}}$ ). Temperature thus continuously decreases from the lower foam to the seed. Even if we will refer only to  $T_{\text{high}}$  in the whole paper, one must keep in mind that when  $T_{\text{high}}$  is increased for a constant TMS flow rate,  $T_{\text{low}}$  increases as well. The difference ( $T_{\text{low}} - T_{\text{high}}$ ) also increases.

**3.2. Limiting Steps of the Growth.** Figure 3 shows the weight gains or losses for the different foams and graphite lid as a function of temperature. TMS and Ar flow rates were kept constant with a TMS/Ar ratio of 0.08.

Three transport domains are evidenced as a function of temperature.

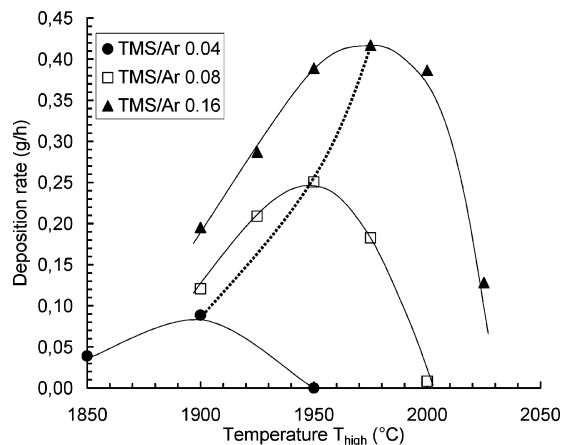


**Figure 4.** Evolution of the deposition rate on the top of the sublimation chamber as a function of the temperature for three TMS/Ar ratios 0.04, 0.08, and 0.16.

(a) **Temperature Range: 1900–1925 °C.** Deposition and/or infiltration occur in foam 1 by the CVD step. Deposition is also observed both on foam 4 and on the graphite lid. As the whole mass transferred to foam 4 did not reach the crucible top, it can be assumed that in this temperature range, the growth is limited by the sublimation step between foam 4 and the graphite lid.

(b) **Temperature Range: 2000 °C and Over.** There is a mass gain in foam 1 and no mass change inside the other foams and on the lid. As no mass gain was measured on the lid, the growth is obviously limited by the feeding step, i.e., the CVD step.

(c) **Temperature Range: 1950–1975 °C.** A mass gain is measured for foam 1 and for the lid. Contrary to case (a), there is no mass gain in foam 4. All the SiC transferred to foam 4 is directly used and transferred to the lid.

Finally, case (a) is observed at low temperature. When the temperature is increased to 2000 °C, the limiting step shifts toward case (b), passing through the intermediate case (c). Similar observations have been done by changing the TMS/Ar ratio. However, the limits between cases (a–c) move to higher temperature when the TMS/Ar ratio is increased.

**3.3. Optimal Deposition Rate.** The deposition rate evolution on the top of the sublimation chamber (graphite lid) is plotted as a function of temperature for three TMS/Ar ratios: 0.04, 0.08, and 0.16 (Figure 4). For each gas-phase composition, the deposition rate passes through a maximum. This maximum moves toward higher temperatures when the TMS/Ar ratio increases. For example, the maximum deposition rate is obtained at about 1900, 1950, and 1975 °C at TMS/Ar ratios of 0.04, 0.08, and 0.16, respectively. The evolution of these maxima is described by the dashed line in Figure 4. Moreover, for each temperature investigated, the deposition rate increases when the TMS/Ar ratio increases.

For each experiment, a global yield of the process has been calculated taking into account the number of moles by hour of SiC formed on the graphite lid  $n(\text{SiC})$  with respect to the molar flow rate of TMS injected into the feeding area  $n(\text{TMS})$ :

$$\text{global process yield} = n(\text{SiC})/n(\text{TMS}) \times 100$$

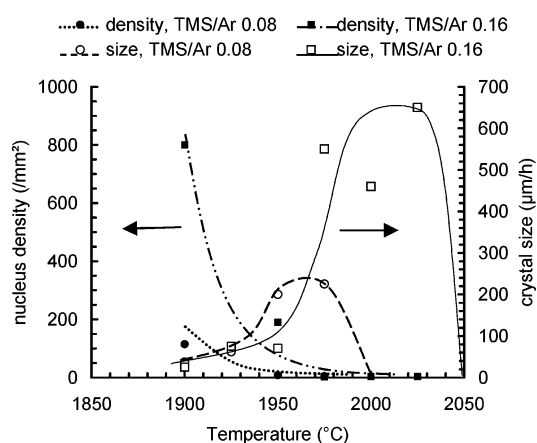


**Figure 5.** Evolution of the nucleus density (the left axis) and the size of the faceted crystals (the right axis) as a function of temperature for two TMS/Ar ratios: 0.08 and 0.16.

For a fixed TMS/Ar ratio, the evolution of the yield with temperature is quite similar to that of the deposition rate. The maximum rate obviously corresponds to the maximum yield. However, when changing the TMS/Ar ratio, the maximum yield reaches 7% for a TMS/Ar ratio of 0.08 and 1950 °C. A further increase of the TMS/Ar ratio leads to a slight decrease of the yield.

**3.4. Nucleation and Growth.** In Figure 5 the nuclei density (left axis) and the size of the faceted crystals (right axis) are presented as a function of temperature for two TMS/Ar ratios: 0.08 and 0.16. It is important to note that for a TMS/Ar ratio of 0.08 and a temperature of 2000 °C, no value is reported as no measurable growth is observed. Both nucleus density and crystal size are thus equal to zero. The same has been obtained at 2050 °C and a TMS/Ar ratio of 0.16. The nuclei density corresponds to the number of crystals per unit area. The crystal size has been measured for the well-faceted crystals per unit time and could thus be assimilated to a crystal growth rate. Only the largest crystals have been taken into account for the size measurement. Those can be assumed to be nucleated in the former time of the experiments.

For a constant TMS/Ar ratio, the growth rate increases when temperature increases and follows an exponential law. For the highest temperatures, the crystal size does not increase any more. The limit of the crystal size, at about 1950 and 1975 °C for TMS/Ar ratios of 0.08 and 0.16, respectively, roughly corresponds to the maxima of deposition rate plotted in Figure 4. In contrast, the nuclei density decreases with increasing temperature. At low temperature, a high density of small crystals is observed. For example, about 800 crystals/mm<sup>2</sup> with a mean size of 25 μm have been obtained at 1900 °C and a 0.16 TMS/Ar ratio. At 2000 °C and with the same TMS/Ar ratio, crystals reach 500 μm in diameter with a density of about 3 mm<sup>-2</sup>. This evolution is illustrated in Figure 6 in which the deposits are formed at (a) 1900 °C, (b) 1950 °C, and (c) 2000 °C with a TMS/Ar ratio of 0.16 during 1 h.

When the TMS/Ar ratio rate is decreased at constant temperature, the nuclei density is strongly reduced and the crystal growth rate increases. In other words, both nucleus density and crystal size curves are shifted to

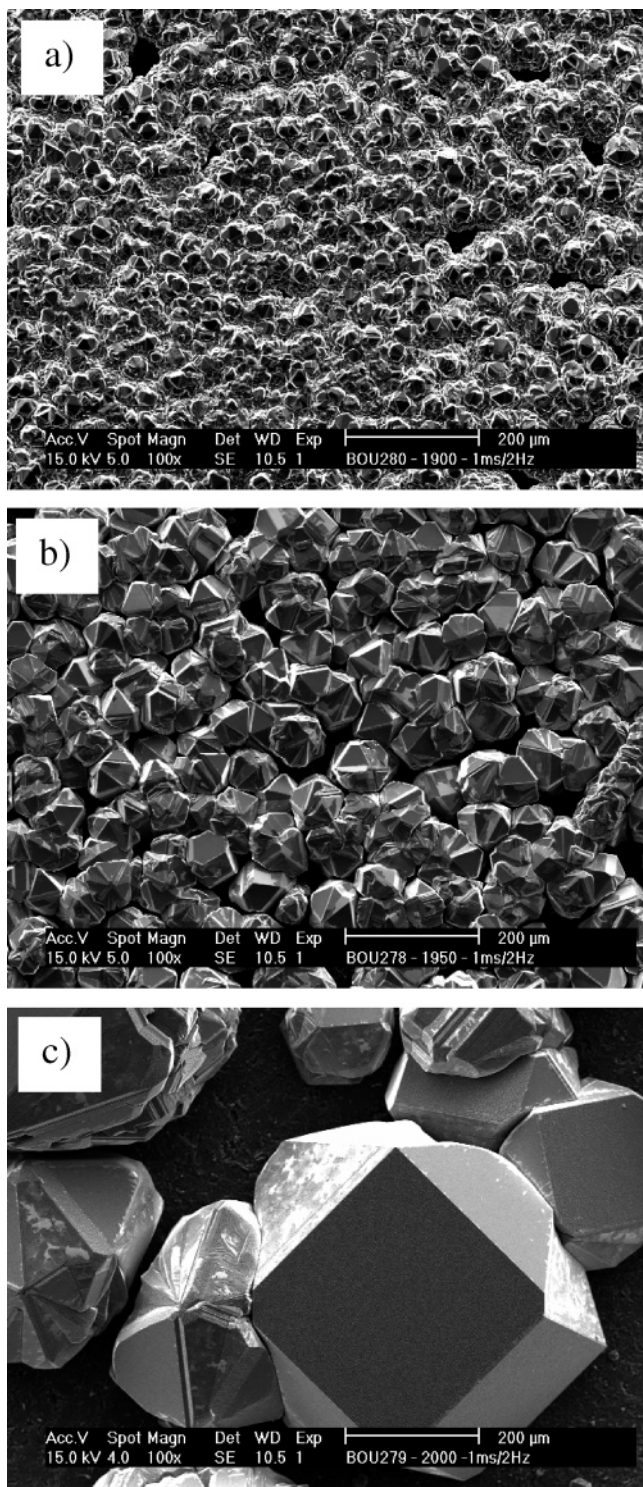


**Figure 6.** SEM pictures of the deposits formed on the graphite lid at (a) 1900 °C, (b) 1950 °C, and (c) 2000 °C with a TMS/Ar ratio of 0.16 during 1 h.

lower temperature with decreasing the feeding gas concentration.

#### 4. Discussion

As a function of experimental conditions, two boundary cases can be evidenced for a chosen TMS flow rate.

(1) At low temperature, the growth is limited by the sublimation step between the source and the seed (case (a)). These conditions are observed for temperatures

lower than the dashed line in Figure 4. In this case, the CF–PVT process can be roughly assimilated to the classical PVT technique. The activation energy related to the growth rate dependence on temperature can be calculated from an Arrhenius law. It is found about 600 kJ/mol, quite close to the activation energy of the SiC sublimation reaction.<sup>15,16</sup> The growth rate on the lid is thus directly correlated to the sublimation rate of the source and should not be modified by changing in the TMS flow rate. Actually, this was not observed as the deposition rate on the lid increases from 0.09 to 0.2 g/h for TMS/Ar ratios of 0.04 and 0.16, respectively. To explain this trend, two parameters have to be taken into account. The first one is the total area of the SiC source. As discussed previously, the growth rate is limited by surface kinetics at the source i.e., SiC deposited in the upper foam, face to the graphite lid. Increasing the TMS/Ar ratio at a constant temperature increases the total amount of the SiC formed in the source and thus increases the “emitting area” of the source. The second parameter is related to the gas-phase composition. We have presented in a previous study<sup>14</sup> based on thermodynamical calculations experiments and simulation of the temperature distribution in the crucible. For a fixed  $T_{\text{high}}$  value, the temperature along the graphite foam was higher when hydrogen instead of argon was used as the carrier gas. As no significant difference in the gas-phase composition between TMS–Ar and TMS–H<sub>2</sub> systems were calculated in the sublimation zone, the higher growth rate obtained with hydrogen has been attributed to changes in the temperature distribution inside the crucible and not to chemical phenomena. In the present work, we can consider that an increase of the TMS/Ar ratio increases the H<sub>2</sub>/Ar ratio due to the decomposition of TMS. From thermodynamics, the decomposition of one mole of TMS liberates more than five moles of hydrogen at 2000 °C. A TMS/Ar ratio of 0.16 would correspond to an H<sub>2</sub>/Ar ratio of 0.8. The hydrogen amount must thus not be neglected. According to these statements, a higher H<sub>2</sub>/Ar ratio would lead to an increase of the source temperature and consequently of the growth rate.

(2) At high temperature, the process is limited by the feeding step, i.e., the CVD deposition and infiltration on the lower part of the source (cases (b) and (c)). As far as both the SiC transfer rate inside the graphite foam and the sublimation rate in the sublimation area are high enough, the growth process is limited by the deposition rate on the lower foam by CVD. These conditions are observed for temperatures higher than or equal to those described by the dashed line in Figure 4. In this range of temperature, the TMS–Ar system leads to SiC and C co-deposition. When the temperature increases, the deposition rate of SiC decreases to zero. This has been observed at 2000 °C and a TMS/Ar ratio of 0.08; only C deposition occurs on the lower foam resulting in no SiC deposition on the lid. These trends are in agreement with those calculated at thermodynamic equilibrium.<sup>17</sup>

The evolution of crystal size and nucleus density as a function of process parameters can give a good estimation of the supersaturation evolution close to the “seed surface”, here the lid. It is well-known that an increase of supersaturation leads to a decrease of the

Gibbs free energy of formation of a nucleus together with the decrease of the critical radius of the nucleus. This means that a higher supersaturation will lead to a higher density of small crystals.<sup>18</sup> According to those simple rules, it can be stated that supersaturation decreases with increasing temperature for a constant TMS flow rate. Supersaturation decreases as well with decreasing the TMS flow rate at a constant temperature.

In the CVD limited conditions, i.e., conditions that belong to the right part of the dashed line in Figure 4, a very small supersaturation can be reached when the deposition rate decreases while the temperature increases. Under such conditions, faceted crystals of 650  $\mu\text{m}$  in diameter were obtained in 1 h with a density close to  $1/\text{mm}^2$ . The growth of SiC very close to equilibrium conditions can thus be expected. If the temperature is further increased, supersaturation falls to zero. When the growth is limited by the sublimation step, i.e., conditions belonging to the left part of the dashed line in Figure 4, it has been evidenced that supersaturation could also be modified by changing the TMS flow rate. However, in this domain, supersaturation is always higher than in the CVD limited regime.

Finally, by a suitable choice of temperature ( $T_{\text{high}}$ ) and TMS/Ar ratio, it is possible to control very simply the supersaturation close to the seed surface.

### 5. Applications

Control of the polytype at high temperatures usually carried out for bulk SiC growth remains a challenge considering the large number of parameters involved in it. Among all, supersaturation and surface energy are of first importance as they influence the nucleation and growth modes. This has been detailed in the reviews.<sup>19,20</sup> Preceding sections are discussed for experiments directly performed on the graphite lid. Lids have been systematically polished in the same way prior to the processing. One can assume to start from the same surface. In other words, the contribution of the graphite surface energy to the nucleation and growth phenomena is similar. In the case of seeded growth, for example, by the use of a SiC single-crystal seed, the seed surface energy contribution to the nucleation and growth phenomena will be different. However, the general trends discussed both for the deposition rate and for the supersaturation evolution with process parameters (temperature and TMS flow rate) would be similar.

In previous works, we have demonstrated the ability of the CF-PVT process to grow a high-purity 0.5-mm-thick 4H-SiC layer starting from an 8° off-axis 4H-SiC substrate<sup>21</sup> and a 0.4-mm-thick 3C-SiC layer on on-axis 4H-SiC seed<sup>22</sup> with the same temperature ( $T_{\text{high}}$ ) of 1950 °C and pressure. The first difference between these two papers is the nucleation step, which has been adapted either to maintain the 4H-SiC polytype via a step-flow growth mode on off-axis seed or to promote the complete 4H-3C heteropolytypic transition via a 2D nucleation mechanism on the terraces. The second difference is the TMS/Ar ratio during the growth period, about 0.06 and 0.12 for the 4H-SiC and the 3C-SiC layers, respectively. This corresponds to growth conditions limited by the CVD step in the 4H case and conditions limited by the sublimation step in the case of 3C. As a consequence,

the growth of 3C-SiC has been performed under higher supersaturation than for 4H-SiC. This is in agreement with the results reported by Fissel.<sup>19</sup> It is worth noting that to our knowledge, with such supersaturation control, we demonstrated for the first time a 30-mm-diameter wafer of (111) oriented 3C-SiC free of double positioning boundaries.

### 6. Conclusion

In the classical sublimation method, the mass transfer and then the supersaturation close to the seed surface are controlled by pressure and temperature distribution within the crucible. In this paper, we have demonstrated that an additional parameter could be of interest for the simple and precise control of the supersaturation in the CF-PVT process: the TMS concentration in the CVD zone. For this, the effect on the deposition rate of both temperature and TMS concentration has been experimentally studied to get a better understanding of mass transfer phenomena within the process. Depending on the conditions, two different regimes were determined. At low temperature and high TMS flow rate, the process is limited by the sublimation step in the growth cavity, corresponding to high supersaturation conditions. At high temperature and low TMS flow rate, the process is limited by the gaseous feeding via CVD, which corresponds to lower supersaturation. Moving across those two regimes by a simple tuning of external parameters (temperature and TMS flow rate) permits a precise adjustment of the supersaturation in the growth chamber. Finally, this study has been applied to the control of the polytype.

**Acknowledgment.** The authors thank NOVASiC for its financial support.

### References

- (1) Muller, S. G.; Glass, R. C.; Hobgood, H. M.; Tsvetkov, V. F.; Brady, M.; Henshall, D.; Malta, D.; Singh, R.; Palmour, J.; Carter, C. H. *Mater. Sci. Eng. B* **2001**, *B80*, 327–331.
- (2) Ohtani, N.; Fujimoto, T.; Katsuno, M.; Aigo, T.; Yashiro, H. *J. Cryst. Growth* **2002**, *237–239*, 1180–1186.
- (3) Anderson, T. A.; Barrett, D. L.; Chen, J.; Elkington, W. T.; Emorhokpor, E.; Gupta, A.; Johnson, C. J.; Hopkins, R. H.; Martin, C.; Kerr, T.; Semenas, E.; Souza, A. E.; Tanner, C. D.; Yoganathan, M.; Zwieback, I. *Mater. Sci. Forum* **2004**, *457–460*, 75–78.
- (4) Hofmann, D.; Bickermann, M.; Eckstein, R.; Kolbl, M.; Muller, S. G.; Schmitt, E.; Weber, A.; Winnacker, A. *J. Cryst. Growth* **1999**, *198/199*, 1005–1010.
- (5) Augustine, G.; Balakrishna, V.; Brandt, C. D. *J. Cryst. Growth* **2000**, *211*, 339–342.
- (6) Nishizawa, S. I.; Kato, T.; Kitou, Y.; Oyanagi, N.; Hirose, F.; Yamaguchi, H.; Bahng, W.; Arai, K. *Mater. Sci. Forum* **2004**, *457–460*, 29–34.
- (7) Nakamura, D.; Gunjishima, I.; Yamaguchi, S.; Ito, T.; Okamoto, A.; Kondo, H.; Onda, S.; Takatori, K. *Nature* **2004**, *430*, 1009–1012.
- (8) Ellison, A.; Magnusson, B.; Son, N. T.; Storasta, L.; Janzen, E. *Mater. Sci. Forum* **2003**, *433–436*, 33–38.
- (9) Chaussende, D.; Baillet, F.; Charpentier, L.; Pernot, E.; Pons, M.; Madar, R. *J. Electrochem. Soc.* **2003**, *150*, G653–G657.
- (10) Yakimova, R.; Syvajarvi, M.; Iakimov, T.; Jacobsson, H.; Raback, R.; Vehanen, A.; Janzen, E. *J. Cryst. Growth* **2000**, *217*, 255–262.
- (11) Wollweber, J.; Rost, H. J.; Schulz, D.; Siche, D. *Mater. Sci. Forum* **2002**, *389–393*, 63–66.
- (12) Anikin, M.; Madar, R. *Mater. Sci. Eng.* **1997**, *46*, 278.

- (13) Takahashi, J.; Ohtani, N.; Kanaya, M. *J. Cryst. Growth* **1996**, *167*, 596–606.
- (14) Auvray, L.; Chaussende, D.; Baillet, F.; Charpentier, L.; Pons, M.; Madar, R. *Mater. Sci. Forum* **2004**, *457–460*, 135–138.
- (15) Kroko, L. *J. Electrochem. Soc.* **1966**, *113*, 801–808.
- (16) Vodakov, Y. A.; Mokhov, E. N.; Ramm, M. G.; Roenkov, A. *D. Cryst. Res. Technol.* **1979**, *14*, 729–740.
- (17) Charpentier, L.; Baillet, F.; Chaussende, D.; Pernot, E.; Pons, M.; Madar, R. *Mater. Sci. Forum* **2003**, *433–436*, 87–90.
- (18) Markov, I. V. In *Crystal Growth for Beginners*; World Scientific: London, 1996.
- (19) Fissel, A. *Phys. Rep.* **2003**, *379*, 149–255.
- (20) Neudeck, P. G.; Powell, J. A. In *Silicon Carbide: Recent Major Advances*; Choyke, W. J., Matsunami, H., Pensyl, G., Eds.; Springer Verlag: New York, 2004; pp 179–205.
- (21) Chaussende, D.; Balloud, C.; Auvray, L.; Baillet, F.; Zielinski, M.; Juillaguet, S.; Mermoux, M.; Pernot, E.; Camassel, J.; Pons, M.; Madar, R. *Mater. Sci. Forum* **2004**, *457–460*, 91–94.
- (22) Chaussende, D.; Latu-Romain, L.; Auvray, L.; Ucar, M.; Pons, M.; Madar, R. *Mater. Sci. Forum* **2005**, *483–485*, 225–228.

CG050009I